



OPEN

Pressure effect on the order–disorder transformation in $L1_0$ FeNi

Li-Yun Tian^{1,2}✉, Olle Eriksson^{2,3} & Levente Vitos^{1,2,4}

The ordered phase of the FeNi system is known for its promising magnetic properties that make it a first-class rare-earth free permanent magnet. Mapping out the parameter space controlling the order–disorder transformation is an important step towards finding growth conditions that stabilize the $L1_0$ phase of FeNi. In this work, we study the magnetic properties and chemical order–disorder transformation in FeNi as a function of lattice expansion by utilizing *ab initio* alloy theory. The largest volume expansion considered here is 29% which corresponds to a pressure of -25 GPa. The thermodynamic and magnetic calculations are formulated in terms of a long-range order parameter, which is subsequently used to find the ordering temperature as a function of pressure. We show that negative pressure promotes ordering, meaning that synthetic routes involving an increase of the volume of FeNi are expected to expand the stability field of the $L1_0$ phase.

Tetragonal FeNi alloy as a candidate permanent magnet material, exhibiting high uniaxial magnetic anisotropy and large magnetic moment, has generated increasing interest^{1–3}, especially since the discovery of single phase tetrataenite (NWA 6259) in 2010. Tetrataenite is a rare-earth-free and low-cost permanent magnet which is expected to be applied widespread in future electromagnetic devices^{4,5}. However, there is the serious problem of the order–disorder transition temperature (320 °C) of tetragonal FeNi, which prevents efficient synthesis routes of this phase, due to the slow atomic diffusion at such a low temperature. Designed to overcome this deficiency, specific tailored synthesis techniques are extremely promising. Techniques that in general increase the order–disorder temperature include the promotion of atomic diffusion, via e.g. atomic vacancies or defects, induced distorted lattice⁶, and third element effect^{7,8}. Modern monatomic layer deposition technique has been used to fabricate $L1_0$ FeNi thin films on a substrate with a small structural match^{1,9}. Unfortunately, this structural realization has decreased long-range order parameter and magnetic anisotropy energy, K_u . Recently, Goto et al. synthesized $L1_0$ FeNi with a high degree of order, of about 0.71 through nitrogen insertion and topotactic extraction (NITE) technology which is the highest degree of order reported so far¹⁰.

As soon as practical synthesis and processing techniques are developed to access the tetrataenite phase in bulk amounts and extend its stability field beyond room temperature, the excellent potential of $L1_0$ FeNi can be realized for permanent magnet applications. Until now, the studies on how to stabilize tetragonal FeNi have been inconclusive. Specifically, there have been few reports that clarify the dependence of the physical properties on volume contraction or expansion. However, it has been confirmed that the chemical and magnetic ordering transitions are interdependent of each other¹¹. In this work we apply a Monte Carlo (MC) method to treat the spin coupled Hamiltonian of the magnetic ordering effects and density functional theory (DFT) to treat the chemical ordering effects.

In our previous work, we have accurately demonstrated an order–disorder transition in $L1_0$ FeNi alloy evaluated from the local atomic rearrangements for chemical ordering¹². Our approach represents an efficient way to describe the ordering transformation based on *ab initio* theory. In the present work, we report the chemical order–disorder transformation and magnetic transition of tetragonal FeNi alloys under various negative pressures. Our goal is to investigate how chemical order–disorder and magnetic transitions change as a function of (negative) pressure, as well as the correlations between magnetic properties and microstructure. The primary

¹Applied Materials Physics, Department of Materials Science and Engineering, Royal Institute of Technology, 100 44 Stockholm, Sweden. ²Division of Materials Theory, Department of Physics and Astronomy, Uppsala University, Box 516, 751 20 Uppsala, Sweden. ³School of Science and Engineering, Örebro University, Örebro, Sweden. ⁴Research Institute for Solid State Physics and Optics, Wigner Research Center for Physics, Budapest 1525, Hungary. ✉email: liyunt@kth.se

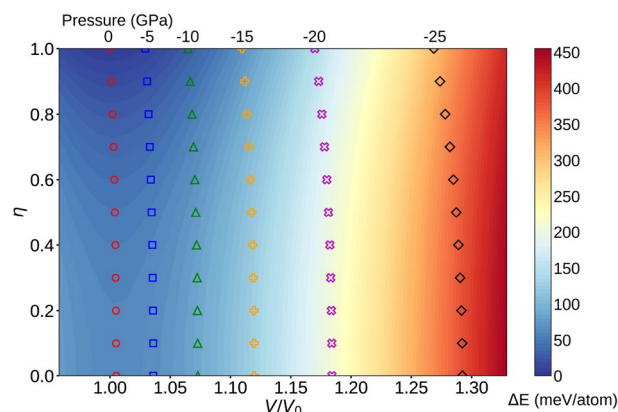


Figure 1. The V/V_0 ratios of tetragonal FeNi alloys corresponding to constant pressures (shown at the top of the figure) as a function of order parameter η . V_0 represents the equilibrium volume of fully ordered FeNi at 0 GPa. The colored symbols show the equilibrium volumes at constant pressure (0, -5, -10, -15, -20 and -25 GPa) as a function of order parameter. The color gradient shows the changes of internal energies relative to the 0 GPa total energy of $L1_0$ FeNi.

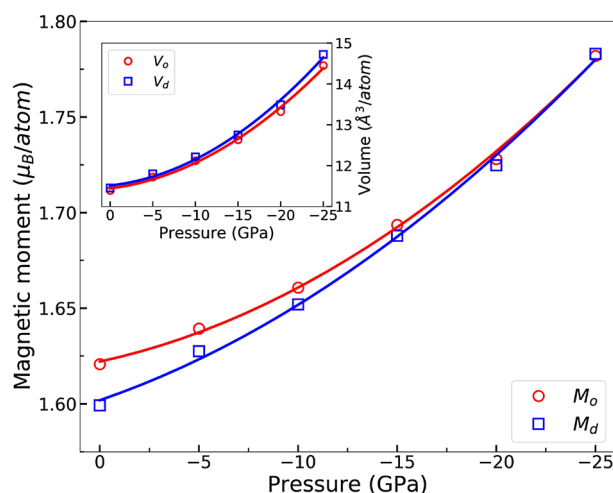


Figure 2. Pressure dependence of the average magnetic moments and volumes (inset) for the fully ordered and disordered FeNi alloys.

conclusion of our investigation is that negative pressure (e.g. chemical volume expansion) is a potential way to increase the order–disorder transition temperature of $L1_0$ FeNi.

Results and discussion

At 0 GPa, the equilibrium volumes and the tetragonal distortions (c/a) of FeNi alloys were obtained by mapping the minimum of the total ground-state energies as a function of long-range order parameter η . The pressure-dependent equilibrium volumes were obtained from the free energies at the corresponding c/a ratios at 0 GPa. Once the corresponding c/a ratios were fixed, the equilibrium volumes of fully and partially ordered FeNi alloys were fitted by the Birch–Murnaghan equation of state^{13,14}. For the external pressure we considered values between 0 and -25 GPa with a step of 5 GPa. We note that the largest negative pressure considered here corresponds approximately to 29% lattice expansion caused by 33.3 at% interstitial N¹⁰.

In Fig. 1, the equilibrium volumes of ferromagnetic FeNi alloys are shown at different ordering states ($0.0 \leq \eta \leq 1.0$) and negative pressures ($-25 \text{ GPa} \leq P \leq 0 \text{ GPa}$) (colored symbols). The color gradient shows the difference of the internal energies at different site occupations relative to the 0 GPa total energy of fully ordered FeNi configuration. It should be observed that at each pressure, the ferromagnetic state is stabilized with increasing long-range order parameter. In addition, the site occupation induced volume change at constant pressure is relatively small. That is because the atomic sizes of Ni and Fe are very similar.

The spin magnetic moments of fully ordered and random FeNi are shown as a function of pressure in Fig. 2. The magnetic moments are calculated by averaging the magnetic moments of Fe and Ni sites in the bct structure. It is well-known that itinerant ferromagnetism is caused by unequal occupancy of the majority-spin and minority-spin in the density of states (DOS). Expanding the atomic volume causes transition between the

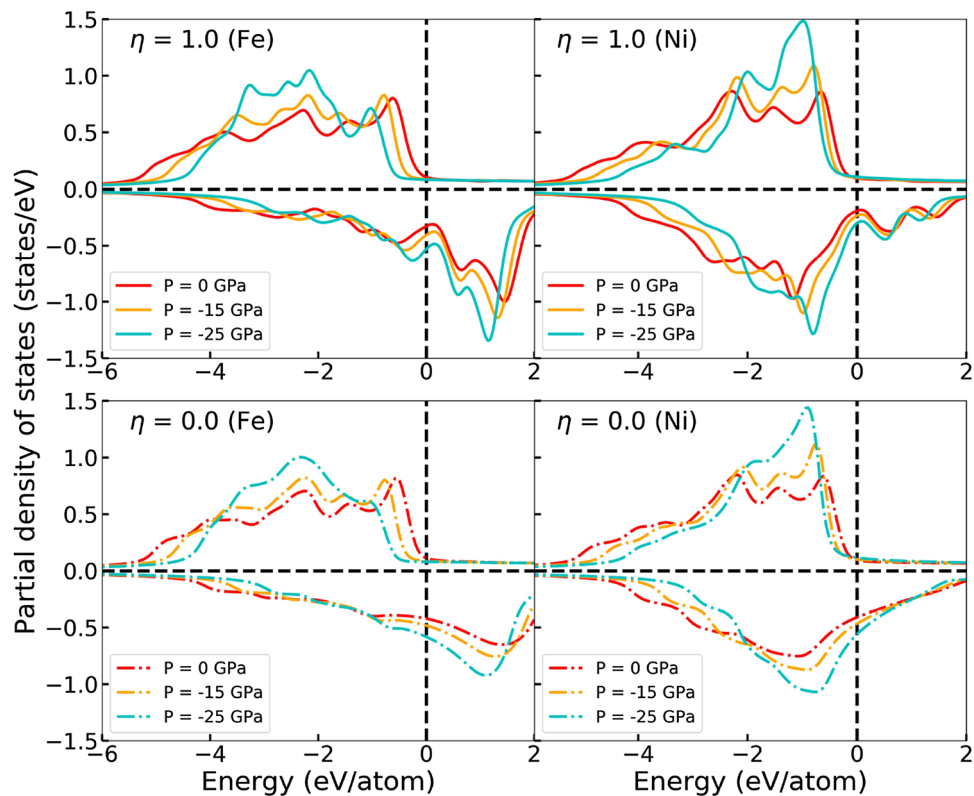


Figure 3. Partial density of states of Fe and Ni for the ordered (up) and random phases (down) at different pressures as a function of energy relative to the Fermi energy.

majority-spin and minority-spin which yields increased magnetic moments. The average magnetic moment of the fully ordered FeNi (M_o) increases from $1.621 \mu_B$ to $1.782 \mu_B$ per atom and that of the fully disordered phase (M_d) from $1.599 \mu_B$ to $1.783 \mu_B$ per atom when the pressure changes from 0 to -25 GPa. The difference between the magnetic moments of tetragonal and random structures becomes smaller with increasing (negative) pressure due to the fact that the volume of random phase V_d is more sensitive to pressure than that of the ordered phase V_o , as shown in the inset of Fig. 2. However, at the same pressures, the magnetic moments of the ordered phases with smaller volumes are slightly larger than those of the corresponding random structures with bigger volumes. This is due to the slightly increased majority-spin and decreased minority-spin in DOS of $L1_0$ FeNi as compared to the random phase¹².

We study the partial DOS of Fe and Ni to understand how the total magnetic moments are formed as a function of negative pressure in Fig. 2. Figure 3 shows that when the pressure becomes more negative, the peaks of both the Fe and Ni DOS become higher and the width of the DOS is decreased. This means that the electrons start to behave in a more localized manner, which is consistent with the fact that negative pressure increases the volume and therefore the electrons in the lattice become more atomic like. For Ni the increasing height and decreasing width of the DOS cancel each other in such a way that the area under the DOS curve, which is the number of states (NOS), up to the Fermi level stays nearly constant for both the spin up and spin down channels. Ni magnetic moment remains therefore almost constant as a function of pressure. For Fe, band narrowing can only be clearly seen in the spin up DOS. Even though changes in the Fe spin down channel are difficult to see, inspecting the NOS reveals that both spin channels undergo pressure induced changes that are roughly the same size, but have the opposite impact on the NOS. The band narrowing effect in the Fe component makes the Fe spin up channel (especially the d partial DOS, not shown) become more saturated which leads to an increase of the magnetic moment. The pressure effect on the DOS is stronger for the random phase due to the larger volume change, meaning that the Fe moment of the random phase grows faster as a function of the negative pressure compared to the ordered case.

The exchange interactions J_{ij} for the ordered and random phases of FeNi for the Fe–Fe, Fe–Ni and Ni–Ni pairs are shown in Fig. 4. The changes in the exchange interaction J_{ij} and local magnetic moment are important for the magnetic free energy and Curie temperature. It is found that the contributions of the exchange interactions are very sensitive to the local environments of the atoms. The strongest interactions are between Fe–Fe pairs at the first nearest neighbor, while the lowest interactions are for Ni–Ni.

Panels (a,b) in Fig. 4 show quite different tendencies for the Fe–Fe pairs at first nearest neighbor distance for the $L1_0$ and random phases. In the $L1_0$ phase, the positive interactions at the first coordination shell are decreased with increasing the volume, while opposite tendency is found for random FeNi. This volume dependence of the exchange parameters is in agreement with Ref.¹⁵.

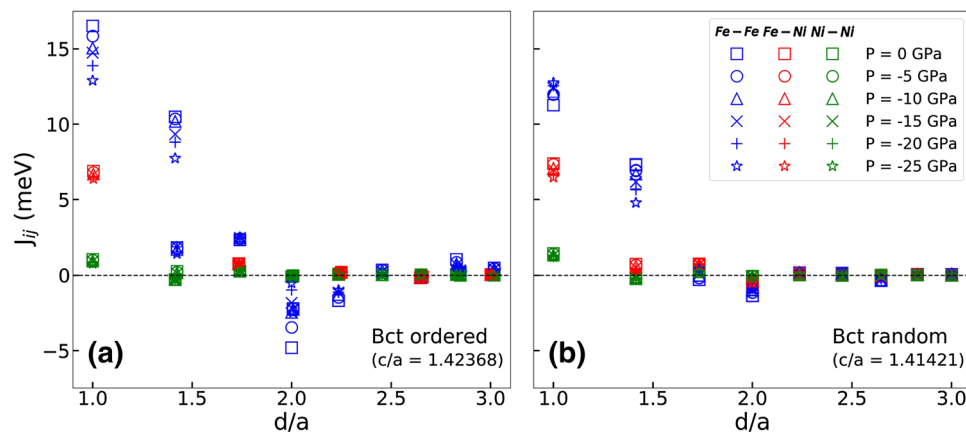


Figure 4. Magnetic exchange interactions between Fe–Fe pairs, Fe–Ni pairs and Ni–Ni pairs in FeNi alloys with tetragonal bct structure (left) and random structure (right) as a function of the distance d/a between the pairs of atoms i and j (a is the lattice constant).

Magnetic moments tend to grow as a function of volume due to the correlation between electrons, which favors parallel spins. Increasing negative pressure typically means decreasing overlap between electronic orbitals. The volume dependency of the orbital overlap integrals will then affect the volume dependency of the J_{ij} parameters. It is not easy to predict how the J_{ij} parameters will change as a function of negative pressure. Ref.¹⁶ found that in pure bcc Fe the pressure dependence of the J_{ij} parameters is very complex. In the ordered $L1_0$ structure, each Fe atom only has four first nearest neighbour Fe atoms, which means that the total first shell Fe–Fe overlapping vanishes quickly. This explains why the first shell Fe–Fe J_{ij} values decrease rapidly as a function of negative pressure. For the random phase the first shell Fe–Fe J_{ij} values are seen to slightly increase, so that at the highest negative pressure the J_{ij} values between the ordered and random cases are comparable in magnitude (≈ 13 meV). This seems reasonable, because at that pressure the magnetic moments of the ordered and random phases are equal (Fig. 2). In general, decreasing J_{ij} interactions should lead to a decreasing Curie temperature. The effect of decreasing J_{ij} and increasing magnetic moments partly cancel each other in the spin Hamiltonian.

Comparing the J_{ij} of ordered and random FeNi phases, we find that the exchange interactions J_{ij} of Ni are not as long ranged as they are for Fe. The Fe–Fe interactions are long ranged, and in the ordered lattice the Fe atoms prefer to form a periodic ferromagnetic coupling. That is why we see a difference in the Fe–Fe exchange interaction magnitudes between the ordered and the random structures. On the other hand, the Ni–Ni and Fe–Ni interactions are short ranged and therefore are less dependent on the degree of order of the structure. This is why the Ni–Ni and Fe–Ni magnitudes are so similar for the two structures. It should be noted that in Fig. 4 the ordered phase has no Fe–Ni (red symbols) interactions for the second nearest neighbour distance, because the ordered $L1_0$ structure is layered in such a way that second nearest neighbour pairs are always the same. The same happens for the fourth nearest neighbours and so on. Additionally, the reason why the ordered phase appears to have two different sets of Fe–Fe interaction parameters is because one set is for Fe–Fe pairs in the same (001) plane and the other set is for Fe–Fe pairs that are separated by a Ni layer. The same is also true for Ni–Ni parameters and higher nearest neighbour pairs.

In Fig. 5, the chemical order–disorder (T_{od}) and magnetic (T_c) transition temperatures are shown as a function of pressure. This is the central result of our investigation. Compared to the volume at 0 GPa, the volume of $L1_0$ FeNi at -25 GPa corresponds to a good approximation to the volume of FeNiN reported by Goto et al.¹⁰. The ab initio theory employed here performs well in reproducing the experimental order–disorder transition temperature at 0 GPa. Most importantly, we find that the chemical ordering temperature is increased with negative pressure. Within the present pressure interval, we find an increased value of the chemical order–disorder transition temperature of approximately 121 K. In addition, the Curie temperatures of $L1_0$ and random FeNi phases vary smoothly with negative pressure.

The changes in the ordering temperature upon negative pressure can be understood by monitoring the components of the Gibbs free energy. Compared to the other effects (vibrational, electronic and magnetic effects), the configurational term ($E_{0K}(V, \eta) - TS_{conf}(\eta) + PV$) is found to have the largest impact on the change of the ordering temperature. We notice that the configurational entropy of fully disordered state remains constant as a function of pressure and hence the change in the ($E_{0K} + PV$) term plays the key role in determining the pressure dependence of the chemical transition temperature. To illustrate this, in Fig. 6 we show the ordering temperatures relative to the zero-pressure ordering temperature. The approximate values are obtained by considering merely the configurational effects ($E_{0K} - TS_{conf}$), adding the pressure term ($E_{0K} - TS_{conf} + PV$), and adding both the pressure and vibrational effects ($E_{0K} - TS_{conf} + F_{vib} + PV$). Their contribution to ordering is different but the internal energy is found to dominate the overall pressure effect. The increase in the internal energy difference with negative pressure in turn is due to the different equations of state for the ordered and disordered phases. Namely, the thermodynamically stable ordered phase has slightly larger bulk modulus, meaning that the ordered phase reaches a particular (negative) pressure level after a smaller volume expansion compared to that of the disordered phase. The substantial internal energy contribution to the increase of T_{od} is reduced by the PV and

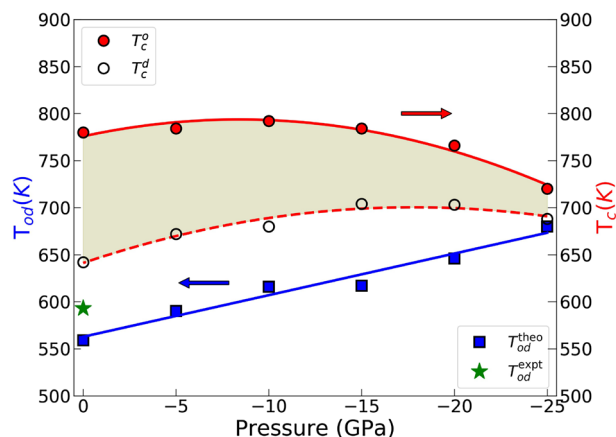


Figure 5. Variation of the order–disorder and magnetic transition temperatures of FeNi with pressure. Open and closed circles show the Curie temperatures of ordered and disordered states, respectively, and squares show the chemical ordering temperature. Experimental ordering temperature is shown for reference¹⁷.

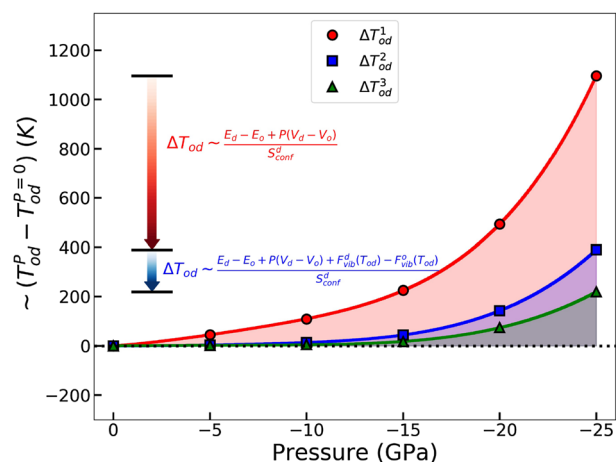


Figure 6. The ordering temperature of FeNi alloy upon negative pressure estimated from fully ordered and disordered states. ΔT_{od} are calculated relative to the ordering temperature at zero pressure. ΔT_{od}^1 considers only the configurational effects on the Gibbs energy ($E_{0K} - TS_{conf}$), ΔT_{od}^2 includes the configurational and PV effects ($E_{0K} - TS_{conf} + PV$), and ΔT_{od}^3 includes the configuration, PV and vibration effects ($E_{0K} - TS_{conf} + PV + F_{vib}$).

vibrational terms to about 219K at -25 GPa. The sum of the electronic entropy and magnetic effects further decrease the pressure-induced transition temperature increment from 219 to 121 K.

The increased ordering temperature in FeNi at negative pressures should promote diffusion. The diffusion near grain boundaries and dislocation-core in FeNi was estimated experimentally and for the activation energy 3.275 eV/atom (~ 316 kJ/mol) was reported¹⁸. Assuming this value at all pressures, we find that the 121K increase of the ordering temperature results in about 3000 times larger diffusion at -25 GPa than at 0 pressure. For a more realistic change of the diffusion upon lattice expansion, however, one should also consider the volume effect on the activation energy, which is neglected in the above estimate.

It is interesting to understand the relationship between Curie temperatures and chemical ordering temperatures. In the present study, the exchange parameters were used to calculate the Curie temperatures at the peaks using the Binder cumulant method¹⁹. This technique has been successfully used in many studies of magnetic materials^{15,20,21}. As seen in Fig. 5, with expanding volume (negative pressure), the changes in J_{ij} lead to a higher T_c in $L1_0$ FeNi and a lower T_c in random phases. This is due to the lower magnetic ground state energy in the ordered phase compared to that in the random phase. Since at very high temperatures the magnetic energy is zero for both phases, the temperature induced change in the magnetic energy must be greater for the ordered phase, which means that the magnetic entropy of the ordered phase must be greater. Additionally, because the magnetic energy increases as a function of temperature, the magnetic contribution to the free energy of FeNi is positive and therefore the magnetic entropy serves to increase the ordering temperature.

Conclusions

In conclusion, we have used first-principles alloy theory and Monte Carlo simulations to analyze the negative pressure effect on the chemical and magnetic ordering transformations of tetragonal FeNi alloys. The results confirm a strong dependence of the transition temperature on negative pressure. The experimental order–disorder transition temperature is accurately reproduced at 0 GPa and the chemical ordering temperature is increased linearly by approximately 121 K with increasing the (negative) pressure from 0 to –25 GPa. This phenomenon is in agreement with the observations made on nitriding the FeNi by NITE technology¹⁰. The insertion of nitrogen in FeNi, results in high degree of long-range order parameter (0.71), which is consistent with the increasing ordering temperature (680 K) at –25 GPa predicted in the present study. We conclude that the pressure-induced ordering temperature in $L1_0$ FeNi is the primary effect to understand the NITE process. By identifying this effect, we delineate a route for synthesizing ordered FeNi alloys for magnetic applications. Our findings contribute to the understanding of the parameter space that controls the order-disorder transformation in this technologically important material, which is significant in order to find growth conditions that stabilize the $L1_0$ phase.

Methods

In order to check the negative pressure behavior, we have undertaken first-principles calculations employing the generalized gradient approximation (GGA) within the exact-muffin-tin orbitals (EMTO) method^{22–24} to evaluate electronic and magnetic properties of tetragonal FeNi alloy. First-principles Gibbs free energy calculations were used to describe the thermodynamic properties of FeNi alloys as a function of a long-range order parameter η . The order parameter is defined as $\eta = 1 - 2x$, where x denotes the mixing between Fe and Ni on the two distinct sites in the $L1_0$ structure ($x = 0$ and $\eta = 1$ is the fully ordered state whereas $x = 0.5$ and $\eta = 0$ is the fully disordered state). The ground-state properties and vibrational and electronic contributions to the Gibbs free energy were computed within the EMTO and magnetic free energy was simulated using the MC approach, as implemented in the Uppsala atomistic spin dynamics (UppASD) program²⁵. The exchange parameters needed in the MC simulations were calculated using EMTO. Details regarding the computational scheme are the same as those used in our previous work¹².

The order–disorder transformation was studied with body-centered tetragonal (bct) crystal structure with two sublattices corresponding to i and j sites. Using the single-site coherent-potential approximation (CPA)^{26,27} to describe the random structures, both i and j sites were occupied by two chemical types of atom. In the process of expanding the volumes of systems with various degrees of chemical order, the tetragonal distortions (c/a) were fixed at the corresponding long-range order structures calculated in our previous work¹².

The Gibbs free energy is considered as a function of temperature T , and pressure P at different long-range order parameter η values:

$$G(T, P, \eta) = E_{0K}(\eta) - TS_{conf}(\eta) + F_{vib}(P, T, \eta) + F_{el}(P, T, \eta) + F_{mag}(P, T, \eta) + PV, \quad (1)$$

where V is the equilibrium volume corresponding to pressure P , E_{0K} is the internal energy per unit

cell at 0 K, $S_{conf}(\eta) = -\frac{k_B}{N} [2 \times (c + \frac{1}{2}\eta) \times \ln(c + \frac{1}{2}\eta) + 2 \times (c - \frac{1}{2}\eta) \times \ln(2 - \frac{1}{2}\eta) + 2 \times (1 - c - \frac{1}{2}\eta) \times \ln(1 - c - \frac{1}{2}\eta) + 2 \times (1 - c + \frac{1}{2}\eta) \times \ln(1 - c + \frac{1}{2}\eta)]$ is the configurational entropy, and F_{vib} , F_{el} and F_{mag} are

the vibrational, electronic and magnetic free energies, respectively. The vibrational free energy $F_{vib}(P, T, \eta)$ was described by Debye model with the Debye temperatures determined from the tetragonal elastic parameters calculated for the ferromagnetic state. The electronic contribution to the free energy was determined by the electronic density of states at the Fermi level. The magnetic contribution to the Gibbs free energy was obtained as $F_{mag} \approx -TS_{mag} \approx -T \frac{\partial (H_{mag})}{\partial T}$ where the Heisenberg Hamiltonian was described as $H_{mag} = -\sum_{i \neq j} J_{ij} \mu_i \mu_j \hat{e}_i \hat{e}_j$ where the exchange interaction J_{ij} and the local magnetic moments μ_i and μ_j on sites i and j were obtained from EMTO calculations.

Received: 19 March 2020; Accepted: 10 June 2020

Published online: 08 September 2020

References

- Kojima, T. *et al.* Fe–Ni composition dependence of magnetic anisotropy in artificially fabricated $L1_0$ -ordered FeNi films. *J. Phys. Condens. Matter* **26**, 064207 (2014).
- Skomski, R. *et al.* Predicting the future of permanent-magnet materials. *IEEE Trans. Magn.* **49**, 3215–3220 (2013).
- Lewis, L. H. *et al.* Inspired by nature: Investigating tetraenaite for permanent magnet applications. *J. Phys. Condens. Matter* **26**, 064213 (2014).
- Lewis, L. H. *et al.* De magnete et meteorite: Cosmically motivated materials. *IEEE Magn. Lett.* **5**, 1–4 (2014).
- Cui, J. *et al.* Current progress and future challenges in rare-earth-free permanent magnets. *Acta Mater.* **158**, 118–137 (2018).
- Frisk, A., Hase, T. P., Svedlindh, P., Johansson, E. & Andersson, G. Strain engineering for controlled growth of thin-film FeNi $L1_0$. *J. Phys. D Appl. Phys.* **50**, 085009 (2017).
- Kojima, T. *et al.* Addition of Co to $L1_0$ -ordered FeNi films: Influences on magnetic properties and ordered structures. *J. Phys. D Appl. Phys.* **47**, 425001 (2014).
- Montes-Arango, A. *et al.* Discovery of process-induced tetragonality in equiatomic ferromagnetic FeNi. *Acta Mater.* **116**, 263–269 (2016).
- Shima, T., Okamura, M., Mitani, S. & Takahashi, K. Structure and magnetic properties for $L1_0$ -ordered FeNi films prepared by alternate monatomic layer deposition. *J. Magn. Magn. Mater.* **310**, 2213–2214 (2007).
- Goto, S. *et al.* Synthesis of single-phase $L1_0$ -FeNi magnet powder by nitrogen insertion and topotactic extraction. *Sci. Rep.* **7**, 13216 (2017).

11. Jena, A. P., Sanyal, B. & Mookerjee, A. Study of the effect of magnetic ordering on order-disorder transitions in binary alloys. *J. Magn. Magn. Mater.* **360**, 15–20 (2014).
12. Tian, L.-Y. *et al.* Density functional theory description of the order-disorder transformation in Fe-Ni. *Sci. Rep.* **9**, 8172 (2019).
13. Murnaghan, F. D. The compressibility of media under extreme pressures. *Proc. Natl. Acad. Sci. U.S.A.* **30**, 244–7 (1944).
14. Birch, F. Finite elastic strain of cubic crystals. *Phys. Rev.* **71**, 809–824. <https://doi.org/10.1103/PhysRev.71.809> (1947).
15. Ruban, A. V., Katsnelson, M., Olovsson, W., Simak, S. & Abrikosov, I. Origin of magnetic frustrations in Fe–Ni Invar alloys. *Phys. Rev. B* **71**, 054402 (2005).
16. Wang, H., Ma, P.-W. & Woo, C. Exchange interaction function for spin-lattice coupling in bcc iron. *Phys. Rev. B* **82**, 144304 (2010).
17. Albertsen, J. Tetragonal lattice of tetraenaite (ordered Fe–Ni, 50–50) from 4 meteorites. *Phys. Scripta* **23**, 301 (1981).
18. Lee, S. *et al.* Formation of FeNi with L1₀-ordered structure using high-pressure torsion. *Philos. Magn. Lett.* **94**, 639–646 (2014).
19. Binder, K. Finite size scaling analysis of Ising model block distribution functions. *Z. Phys., B. Condens. Matter* **43**, 119–140 (1981).
20. Huang, S. *et al.* Mechanism of magnetic transition in FeCrCoNi-based high entropy alloys. *Mater. Des.* **103**, 71–74 (2016).
21. Edström, A., Chico, J., Jakobsson, A., Bergman, A. & Ruzs, J. Electronic structure and magnetic properties of L1₀ binary alloys. *Phys. Rev. B* **90**, 014402 (2014).
22. Vitos, L., Skriver, H. L., Johansson, B. & Kollár, J. Application of the exact muffin-tin orbitals theory: The spherical cell approximation. *Comput. Mater. Sci.* **18**, 24–38 (2000).
23. Vitos, L., Abrikosov, I. & Johansson, B. Anisotropic lattice distortions in random alloys from first-principles theory. *Phys. Rev. Lett.* **87**, 156401 (2001).
24. Vitos, L. *Computational Quantum Mechanics for Materials Engineers: The EMTO Method and Applications* (Springer, New York, 2007).
25. Skubic, B., Hellsvik, J., Nordström, L. & Eriksson, O. A method for atomistic spin dynamics simulations: Implementation and examples. *J. Phys. Condens. Matter* **20**, 315203 (2008).
26. Soven, P. Coherent-potential model of substitutional disordered alloys. *Phys. Rev.* **156**, 809 (1967).
27. Gyorffy, B. Coherent-potential approximation for a nonoverlapping-muffin-tin-potential model of random substitutional alloys. *Phys. Rev. B* **5**, 2382 (1972).

Acknowledgements

The work was supported by the Swedish Research Council (VR), the Swedish Foundation for Strategic Research (SSF), the Carl Tryggers Foundations, the Swedish Innovation Agency (VINNOVA), the Hungarian Scientific Research Fund (OTKA 128229), the Swedish Energy Agency, eSENCE and STandUPP. The computations were performed on resources provided by the Swedish National Infrastructure for Computing (SNIC) at Linköping.

Author contributions

L. T. performed the calculations, analysed the data and wrote the manuscript; L. V. conceived and supervised the work; L. V. and O. E. discussed the results and commented on the manuscript.

Funding

Open access funding provided by Royal Institute of Technology.

Competing interests

The authors declare no competing interests.

Additional information

Correspondence and requests for materials should be addressed to L.-Y.T.

Reprints and permissions information is available at www.nature.com/reprints.

Publisher's note Springer Nature remains neutral with regard to jurisdictional claims in published maps and institutional affiliations.



Open Access This article is licensed under a Creative Commons Attribution 4.0 International License, which permits use, sharing, adaptation, distribution and reproduction in any medium or format, as long as you give appropriate credit to the original author(s) and the source, provide a link to the Creative Commons license, and indicate if changes were made. The images or other third party material in this article are included in the article's Creative Commons license, unless indicated otherwise in a credit line to the material. If material is not included in the article's Creative Commons license and your intended use is not permitted by statutory regulation or exceeds the permitted use, you will need to obtain permission directly from the copyright holder. To view a copy of this license, visit <http://creativecommons.org/licenses/by/4.0/>.

© The Author(s) 2020